

PSEUDO FOUR-CHANNEL IMAGE DENOISING FOR NOISY CFA RAW DATA

Hiroki Akiyama, Masayuki Tanaka, and Masatoshi Okutomi

Tokyo Institute of Technology

ABSTRACT

Most demosaicking algorithms only focus on handling noise-free CFA raw data. In practice, the CFA raw data are corrupted by noise, which degrades demosaicking performance. Full-color image quality strongly depends on the performance of the demosaicking. Here, we propose a CFA raw data denoising algorithm. In the proposed algorithm, the CFA raw data is converted to a pseudo four-channel image by rearranging pixels. Then, the four-channel data are transformed based on the principal component analysis (PCA). Existing high-performance gray image denoising algorithm is applied to each transformed image. Finally, the denoised data is rearranged to obtain denoised CFA raw data. We evaluate both the denoised CFA raw data as well as the full-color image reconstructed with the noisy CFA raw data. Experimental comparisons demonstrate that the proposed algorithm outperforms existing state-of-the-art algorithms.

Index Terms— Demosaicking, Denoising, Bayer-CFA, PCA

1. INTRODUCTION

A single image sensor with a color filter array (CFA) is widely used for a color image acquisition and the most common pattern is the Bayer pattern CFA [1]. The data acquired by the single image sensor with the CFA is called CFA raw data.

In order to reconstruct a full-color image from the CFA raw data, we need to estimate the other two missing color pixel values. This estimation process is called demosaicking. Many demosaicking algorithms have been proposed in many literatures [2, 3, 4, 5, 6, 7].

Most demosaicking algorithms only focus on handling the noise-free CFA raw data. However, in practice, we need to take account of the noise added to the CFA raw data. In the presence of noise, the performance of the demosaicking algorithm degrades drastically. Consequently, severe color artifacts appear in the full-color image demosaicked with the noisy CFA raw data.

There are three approaches to generate the full-color image from the noisy CFA raw data. A straightforward approach is denoising-after-demosaicking, where demosaicking and denoising are sequentially applied. Many high-performance demosaicking algorithms for the noise-free CFA raw data

are existing. Many effective denoising algorithms assuming additive white Gaussian noise (AWGN) have also been proposed [15, 16]. But their simple combination provides poor results. One reason is that the demosaicking process changes the statistical properties of the noise. The removal of non-AWGN is a very challenging problem.

The second approach is denoising-before-demosaicking. If we can sufficiently reduce the noise of the CFA raw data before the demosaicking process, we can simply apply the demosaicking algorithm for the noise-free CFA raw data to the denoised CFA raw data. However, most high-performance denoising algorithms are designed for a normal gray or full-color image. We cannot get the high-performance by directly applying those denoising algorithms to reduce the noise of the CFA raw data because of the underlying mosaic structure of the CFA. Therefore, we need to design a denoising algorithm for noisy CFA raw data as well as some CFA denoising algorithms [8, 9, 10].

The third approach is joint denoising and demosaicking [11, 12, 13, 14]. These algorithms of this approach tend to be complicated and require a huge computational cost.

In this paper, we propose a novel CFA raw data denoising algorithm. In the proposed CFA raw data denoising, the CFA raw data is first divided into four sub-images. Since the set of sub-images can be regarded as a four-channel color image, we call it *pseudo four-channel image*. In order to improve the denoising performance, the *color* space of the pseudo four-channel image is transformed based on the principal component analysis (PCA). Then, existing high-performance denoising algorithm is applied to the pseudo four-channel image in the transformed domain. The denoised pseudo four-channel image is restored back to the CFA raw data. Finally, the full-color image is generated with the denoised CFA raw data by using an existing high-performance demosaicking algorithm [5].

A similar approach, i.e. dividing into four sub-images and denoising them, was proposed by Park et al. [10]. Our proposed method outperforms it due to two mechanisms: adaptive color transformation and block artifact reduction which are explained in the following sections.

We evaluate the performance of the CFA raw data denoising and the final full-color image quality reconstructed with the noisy CFA raw data. Experimental comparisons demonstrate that the proposed algorithm outperforms state-of-the-art

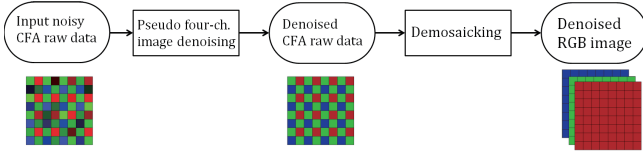


Fig. 1. The image processing pipeline of the denoising-before-demosaicking

algorithms.

2. DENOISING AND DEMOSAICKING

The noisy CFA raw data \mathbf{y} can be expressed as

$$\mathbf{y} = \mathbf{M}\mathbf{x} + \mathbf{n}, \quad (1)$$

where \mathbf{x} is the vector representation of the noise-free RGB image, \mathbf{M} is the matrix which represents sub-sampling operation according to the CFA pattern, and \mathbf{n} is the noise. In this paper, we assume the noise is signal independent Gaussian noise with zero-mean. The variance of the noise depends on the channel. The variances of R, G, and B channels are denoted as σ_R^2 , σ_G^2 , and σ_B^2 , respectively.

Let $\mathbf{D}_n(\cdot)$ and $\mathbf{D}_m(\cdot)$ denote the denoising and the demosaicking processes, respectively. Those processes may be a non-linear process. The full-color image generated by the denoising-after-demosaicking approach can be expressed by

$$\hat{\mathbf{x}} = \mathbf{D}_n(\mathbf{D}_m(\mathbf{M}\mathbf{x} + \mathbf{n})). \quad (2)$$

The error after demosaicking is

$$\boldsymbol{\eta} = \mathbf{D}_m(\mathbf{M}\mathbf{x} + \mathbf{n}) - \mathbf{x}. \quad (3)$$

If this error is AWGN, the denoising algorithm can effectively reduce the noise. However, the error is not the AWGN because the demosaicking process is usually a non-linear operation. Non AWGN noise removal is a challenging problem.

The full-color image generated by the denoising-before-demosaicking approach can be expressed by

$$\hat{\mathbf{x}} = \mathbf{D}_m(\mathbf{D}_n(\mathbf{M}\mathbf{x} + \mathbf{n})). \quad (4)$$

If CFA raw data denoising can efficiently reduce the noise of the noisy CFA raw data, we can simply apply the demosaicking algorithm which assumes the noise-free CFA raw data.

3. PSEUDO FOUR-CHANNEL IMAGE DENOISING

3.1. Image processing pipeline

The overall image processing pipeline from the noisy CFA raw data to the full-color image is shown in Fig. 1. In the proposed pseudo four-channel image denoising, first, we decompose the noisy CFA raw data into four sub-images. The four sub-images can be considered as one pseudo four-channel image. We can generate four different types of pseudo four-channel images, namely, a GRBG-channel image, an RGGB-channel image, a BGGR-channel image, and a GBRG-channel image. Each pseudo four-channel image is

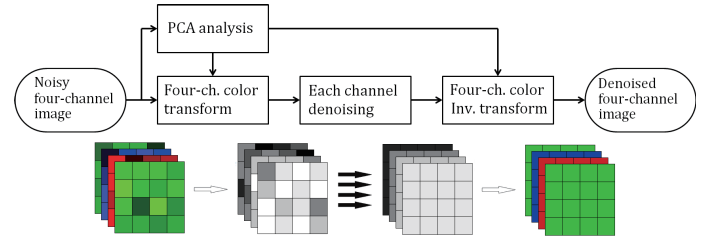


Fig. 2. Four-channel image denoising.

denoised in the transformed domain as shown in Fig. 2. The denoised four-channel images are rearranged and averaged to generate the denoised CFA raw data. The averaging process can effectively reduce block artifacts caused by a block structure of the sub-image division. Finally, the existing demosaicking algorithm is applied to the denoised CFA raw data to obtain the full-color image.

3.2. Four-channel image denoising with adaptive color transformation

Each pixel of the pseudo four-channel image like the GRBG-channel image has four-channel data, namely, G_1 , R, B, and G_2 . Although this data does not represent color, we call this data the color with analogy of the RGB-channel image. It is empirically known that the transformation of the color data into the principal component space helps denoising process because the signal energy is compact while the noise is distributed equally in all dimensions. Park et al heuristically proposed the transformation derived with off-the-shelf color transformation [10]. In this paper, we adaptively derive the transformation based on the PCA of the input noisy CFA raw data. For the PCA of the noisy data, we follow the same manner as in [9]. The covariance matrix of the noisy pseudo four-channel image is calculated as

$$\tilde{\mathbf{X}} = [\mathbf{x}_1 + \mathbf{n}_1 \quad \mathbf{x}_2 + \mathbf{n}_2 \quad \cdots \quad \mathbf{x}_n + \mathbf{n}_n], \quad (5)$$

$$\tilde{\boldsymbol{\Sigma}} = \frac{1}{n-1} (\tilde{\mathbf{X}} - \boldsymbol{\mu})(\tilde{\mathbf{X}} - \boldsymbol{\mu})^T, \boldsymbol{\mu} = \frac{1}{n} \sum_{i=1}^n \mathbf{x}_i, \quad (6)$$

where \mathbf{x}_i is the four-channel data at i -th pixel, \mathbf{n}_i is the noise at i -th pixel, and T represents the transpose operator. Assuming that the signal and the noise are uncorrelated, we can estimate the covariance matrix of the signal as

$$\boldsymbol{\Sigma} = \tilde{\boldsymbol{\Sigma}} - \text{diag} \left([\sigma_1^2 \quad \sigma_2^2 \quad \sigma_3^2 \quad \sigma_4^2]^T \right), \quad (7)$$

where $\text{diag}(\mathbf{z}_i)$ represents the diagonal matrix composed of the elements of \mathbf{z}_i , and σ_k^2 is the variance of the k -th channel of the pseudo four-channel image. For the GRBG-channel image, $[Y_1 \ Y_2 \ Y_3 \ Y_4]^T = \mathbf{P}[G_1 \ R \ B \ G_2]^T$. The transformation matrix \mathbf{P} can be expressed with the eigen vectors \mathbf{v}_k of the covariance matrix $\boldsymbol{\Sigma}$ as

$$\mathbf{P} = [\mathbf{v}_1 \quad \mathbf{v}_2 \quad \mathbf{v}_3 \quad \mathbf{v}_4]^T. \quad (8)$$

We can transform the four-channel data into the principal component space by multiplying the transformation matrix.

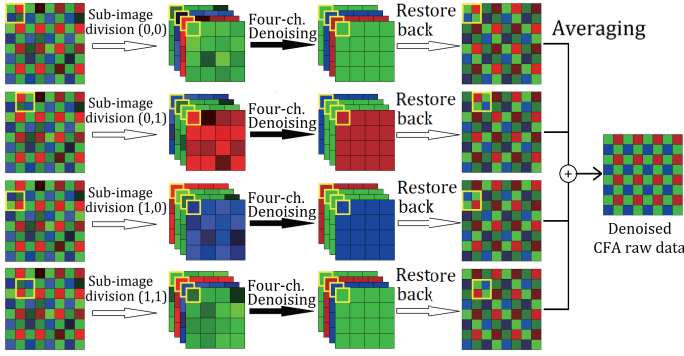
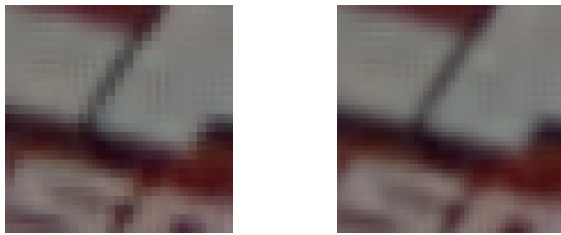


Fig. 3. The process flow of block artifact reduction.



(a) without the block reduction (34.49dB). (b) with the block reduction (35.28dB).

Fig. 4. The difference between with and without the block reduction ($\sigma = 20$).

The variance of the noise in the k -th principal component can be estimated as

$$\sigma_{Y_k}^2 = P_{1k}^2 \sigma_G^2 + P_{2k}^2 \sigma_R^2 + P_{3k}^2 \sigma_B^2 + P_{4k}^2 \sigma_G^2. \quad (9)$$

Each transformed pseudo four-channel image is denoised by an existing high-performance gray-image denoiser with the estimated noise variance.

3.3. Block artifact reduction

A single pixel of the pseudo four-channel image corresponds to the four-pixel block in the CFA raw data. Therefore, it causes block artifacts in the demosaicked full-color image. In order to reduce the block artifacts, we average four different types of the pseudo four-channel images as shown in Fig. 3. By changing the start position of the four-pixel block in the CFA raw data, we can generate four different types of the pseudo four-channel images: the GRBG-channel image, the RGGB-channel image, the BGGR-channel image, and the GBRG-channel image. The four-pixel blocks of each pseudo four-channel image overlap each other in the CFA raw data. This is why the averaging process can reduce the block artifacts. Fig. 4 shows the effect of block artifact reduction.

4. EXPERIMENTAL RESULTS

In order to evaluate the proposed algorithm¹, we conducted two types of experiments. First experiment is the comparison

¹The matlab code of our proposed algorithm can be down- loaded from <http://www.ok.ctrl.titech.ac.jp/res/CFADN/CFADN.html>

Table 1. The average PSNRs of 24 CFA raw data denoising from the Kodak dataset, where the bold font represents the best performance in each noise level.

σ	[16] to CFA	[9]	[10]	proposed
5	40.11	39.54	39.49	40.06
10	37.33	36.39	36.94	37.58
15	35.50	34.32	35.54	36.16
20	34.04	32.74	34.51	35.12
30	31.76	30.36	32.90	33.45
40	29.96	28.57	31.49	31.97

of the CFA raw data denoising performance without the demosaicking process. The Peak Signal-to-Noise Ratio (PSNR) between the denoised CFA raw data and the ground-truth data are evaluated.

We also compare the full-color image reconstruction performance from the noisy CFA raw data. For the quantitative comparisons, the color PSNR (CPSNR) between the full-color image reconstructed with the noisy CFA raw data and the ground-truth full-color image is calculated.

We use high-resolution Kodak dataset which includes 24 2048x3072 sized images. In the proposed algorithm, we use the BM3D [16] for the gray image denoising and the residual interpolation [5] for the color demosaicking.

4.1. Comparisons of CFA raw data denoising

We compare the proposed algorithm with the direct BM3D [16], PCASAD [9] and Park's algorithm [10]. The direct BM3D denoises the CFA raw data, assuming that the CFA raw data is the gray image. The BM3D [16] is used for the gray image denoising of the Park's algorithm [10] as well as the proposed algorithm.

Table 1 shows the numerical comparisons of CFA raw data denoising. This comparison demonstrates that the proposed algorithm outperforms other existing algorithms in almost all noise levels.

4.2. Comparisons of full-color image reconstruction

Here, we evaluate the performance of the full-color image reconstruction from the noisy CFA raw data. We compare the proposed algorithm with existing algorithms; the combination of CFA denoising as mentioned above and demosaicking, joint denoising and demosaicking including LPAICI [12], JDDTV [13], and LSLCD [14]. Comparison algorithms also include demosaicking only and simple denoising-after-demosaicking method, namely, the straightforward combination of demosaicking and gray-scale denoiser.

Table 2 and Fig. 6 show the average CPSNRs of data set images. This comparison demonstrated that the proposed algorithm outperforms existing algorithms. A visual comparison is shown in Fig. 5. It shows that the proposed algorithm effectively suppresses color artifacts.

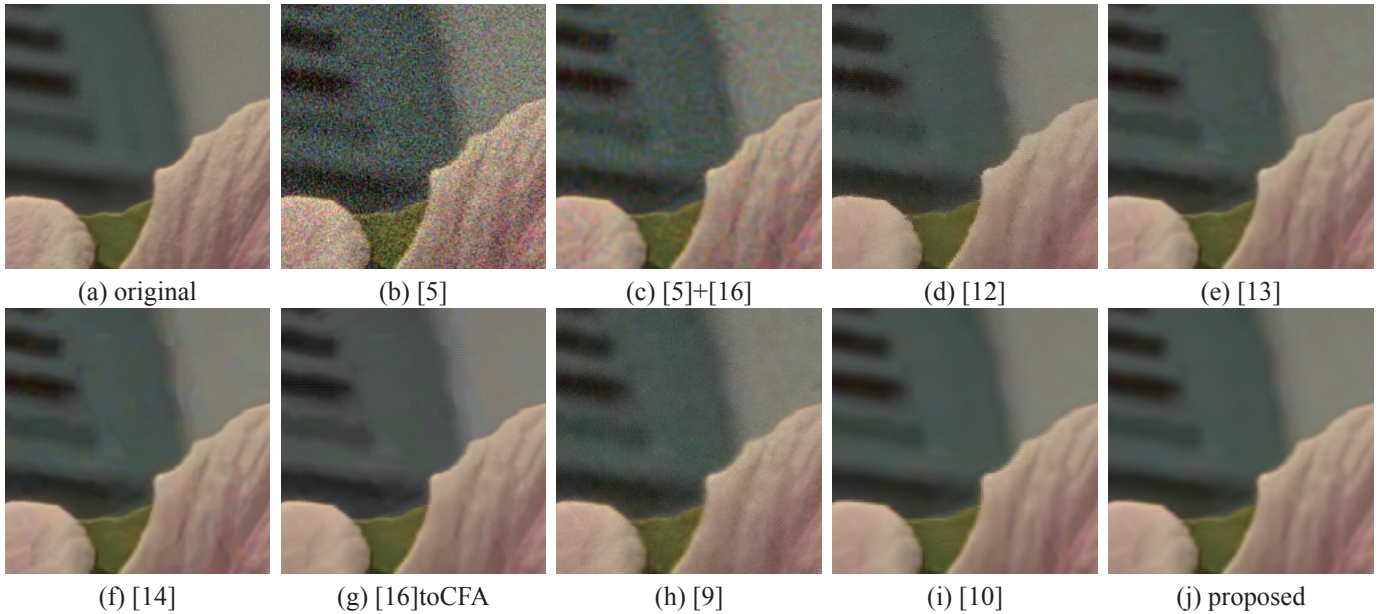


Fig. 5. Visual comparison using the Kodak high resolution image dataset ($\sigma = 20$).

Table 2. The average CPSNRs of 24 images of the Kodak dataset, where the bold font represents the best performance in each noise level.

Type	Dm		Joint Dn and Dm					Dn \rightarrow Dm [5]		
	[5]	[5] + [16]	[12]	[13]	[14]	[16]toCFA	[9]	[10]	proposed	
σ										
5	34.84	38.76	38.48	38.99	39.01	39.48	39.13	39.07	39.52	
10	29.35	35.38	35.81	36.80	36.67	36.97	36.38	36.78	37.32	
15	26.01	32.92	34.16	35.40	35.26	35.17	34.49	35.41	35.99	
20	23.63	30.99	32.93	34.35	34.12	33.68	33.01	34.46	34.98	
30	20.32	28.10	31.01	32.62	N/A [†]	31.33	30.74	32.81	33.35	
40	18.04	26.00	29.47	31.12	N/A [†]	29.46	29.00	31.41	31.89	

[†] [14] only supports noise level up to 20.

5. CONCLUSION

We have proposed the simple and the effective CFA denoising algorithm. The adaptive color transformation and the block artifact reduction can effectively improve the performance. The experiments proved that the proposed algorithm can reconstruct full-color images, suppressing the noise in the CFA raw data.

6. REFERENCES

- [1] B. Bayer, "Color imaging array," U.S. Patent 3971065, 1976.
- [2] L. Zhang and X. Wu, "Color demosaicking via directional linear minimum mean square-error estimation," IEEE Trans. on Image Processing, vol. 14, no. 12, pp. 2167–2178, 2005.
- [3] X. Li, B. Gunturk, and L. Zhang, "Image Demosaicing: A Systematic Survey," Proc. SPIE Electronic Imaging, vol. 6822, pp. 68221, 2008.
- [4] L. Zhang, X. Wu, A. Buades, and X. Li, "Color demosaicking by local directional interpolation and nonlocal adaptive thresholding," Journal of Electronic Imaging, vol. 20, no. 2, pp. 023016–023016, 2011.
- [5] D. Kiku, Y. Monno, M. Tanaka, and M. Okutomi, "Residual Interpolation for Color Image Demosaicking," Proc. of IEEE Int. Conf. on Image Processing (ICIP), pp. 2304–2308, 2013.

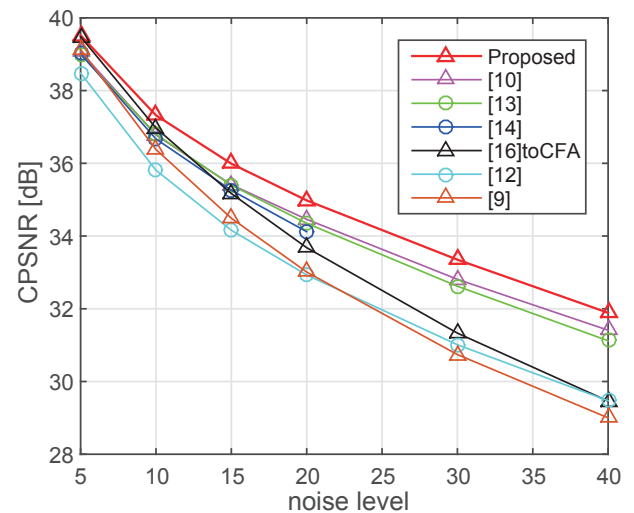


Fig. 6. The comparison of CPSNRs in different noise levels.

- [6] D. Kiku, Y. Monno, M. Tanaka, and M. Okutomi, "Minimized-Laplacian residual interpolation for color image demosaicking," *Proc. SPIE Electronic Imaging*, vol. 9023, pp. 90230L-1–8, 2014.
- [7] D. Kiku, Y. Monno, M. Tanaka, and M. Okutomi, "Adaptive Residual Interpolation for Color Image Demosaicking," *Proc. of IEEE Int. Conf. on Image Processing (ICIP)*, 2015.
- [8] A. Danielyan, M. Vehvilainen, A. Foi, V. Katkovnik, and K. Egiazarian "Cross-color BM3D filtering of noisy raw data," in *Proc. International Workshop on Local and Non-Local Approximation in Image Processing LNLA*, pp. 125–129, 2009.
- [9] L. Zhang, R. Lukac, X. Wu, and D. Zhang, "PCA-based spatially adaptive denoising of CFA images for single-sensor digital cameras," *IEEE Trans. on Image Processing*, vol. 18, no. 4, pp. 797–812, 2009.
- [10] S. H. Park, H. S. Kim, S. Linsel, M. Parmar, and B. A. Wandell, "A case for denoising before demosaicking color filter array data *Asilomar Conf. on Signals, Systems, and Computers*, pp. 860–864, 2009.
- [11] K. Hirakawa, and T.W. Parks, "Joint demosaicing and denoising *Image Processing*," *IEEE Trans. on Image Processing*, vol. 15, no. 8, pp. 2146–2157, 2006.
- [12] D. Paliy, V. Katkovnik, R. Bilcu, S. Alenius, and K. Egiazarian, "Spatially Adaptive Color Filter Array Interpolation for Noiseless and Noisy Data," *Int. J. Imaging Sys. Tech., Sp. Iss. Appl. Color Image Process.*, vol. 17, no. 3, pp. 105–122, 2007.
- [13] L. Condat, and S. Mosaddegh, "Joint demosaicking and denoising by total variation minimization," *Proc. of IEEE Int. Conf. on Image Processing (ICIP)*, pp. 2781–2784, 2012.
- [14] E. Dubois, and G. Jeon, "Demosaicking of Noisy Bayer-Sampled Color Images With Least-Squares Luma-Chroma Demultiplexing and Noise Level Estimation," *IEEE Trans. on Image Processing*, vol. 22, no. 1, pp. 146–156, 2013.
- [15] J. Mairal, F. Bach, J. Ponce, G. Sapiro, and A. Zisserman, "Non-local sparse models for image restoration." *IEEE Int. Conf. on Computer Vision (ICCV)*, pp.2272–2279, 2009.
- [16] K. Dabov, A. Foi, V. Katkovnik, and K. Egiazarian, "Image denoising with block-matching and 3D filtering," *Proc. SPIE Electronic Imaging*, no. 6064A–30, 2006.